Fullwave Analysis of Bilateral Microwave Structures on Multilayered Uniaxially Anisotropic Substrates

M.L. TOUNSI [1], R. TOUHAMI [1], and M.C.E. YAGOUB [2]

[1] Instrumentation Laboratory, Faculty of Electronics and Informatics
U.S.T.H.B University.
P.O Box 32. El-Alia. Bab-Ezzouar, 16111, Algiers
ALGERIA

[2] School of Information Technology and Engineering
University of Ottawa
800 King Edward Ave, Ottawa, Ontario, K1N 6N5
CANADA

Abstract: - The spectral-domain method is applied to the analysis of the dispersive properties of the multilayered bilateral microwave structures printed on uniaxial anisotropic substrates. An alternative formulation of dyadic Green's function is derived for bilateral microwave structures in an automatic way via a recursive process. The number of dielectric layers is arbitrary. Numerical results describing the propagation characteristics are presented and discussed for both electric and magnetic wall symmetries. It is found that certain structures have a very weak dispersion. This low dispersion feature signifies the fact that the quasi-static analysis is adequate for designing practical microwave and millimeter-wave circuits.

Key-Words: - Anisotropic substrate, multilayered microwave circuits, fullwave analysis, spectral domain approach, Galerkin method.

1. Introduction

Accurate knowledge of the propagation parameters of printed lines plays a vital role in the design of modern microwave and millimeter-wave integrated circuits. Planar transmission lines with anisotropic dielectric substrates offer wide possibilities in MIC applications [1]-[3]. Anisotropy is introduced unintentionally during the manufacturing process, or deliberately in order to obtain non-reciprocal devices, radar absorbers or serve to improve circuit performance. Neglecting this anisotropy induces errors during the design. Hence, rigorous dynamic techniques must be applied in order to get an accurate solution to secure the design and improve the CAD models.

In this paper, effects of substrate anisotropy on the dispersion properties of multilayer bilateral microwave structures are investigated. The number of dielectric layers is arbitrary. The spectral-domain method (SDM) [4], is employed to derive the dyadic admittance Green's functions. The (SDM) method procures a good compromise between efficiency, CPU time and memory requirements.

A set of well-behaved basis functions are chosen to expand the current density on the strips, and the Galerkin method is used to find a matrix system of linear equations, whose determinant contains the propagation constant. Specially, two kinds of symmetries (electric and magnetic walls) are considered, with numerical data provided for both. Very good agreement between the calculated results and those available in the literature is found for open as well as shielded structures. It is found that certain structures have a very weak dispersion. This characteristic is very useful since a simple quasi-static approach can be employed for accurate circuit designs in the high-frequency region. Further, the weak dispersion property is indeed very attractive for wide-band applications for designing practical microwave and millimeter-wave circuits.

2. Formulation of the method

The structure under analysis is a general bilateral microwave structure printed on multilayered anisotropic layers whose transverse section is depicted in fig. 1. The structure is enclosed in a perfectly conducting channel and assumed to be uniform in the z direction. All dielectric layers are assumed anisotropic and lossless.
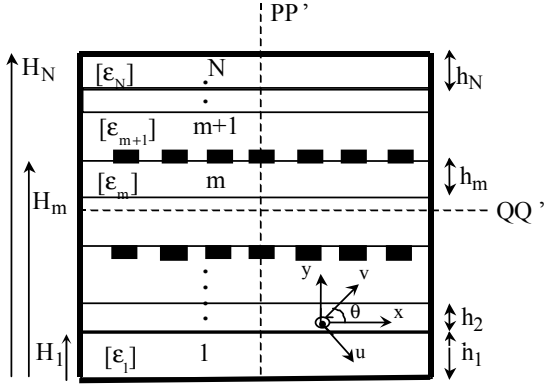
Fig. 1 View of the multilayer anisotropic structure

In view of the symmetry with respect to the planes PP' and QQ', we only need to consider four propagation modes:

Even-even: PP' magnetic wall, QQ' magnetic wall.
Even-odd : PP' magnetic wall, QQ' electric wall.
Odd-even: PP' electric wall, QQ' magnetic wall.
Odd-odd: PP' electric wall, QQ' electric wall.

Thus, to compute the dispersive properties of this structure, it is sufficient to analyze only one quarter of the structure with appropriate boundary conditions corresponding to the four different modes. The even- and odd-modes correspond to an open-circuit [magnetic wall (MW)] and a short-circuit [electrical wall (EW)], respectively. The dielectric layers shown in Fig. 1 are modelled by using a diagonal relative tensor $[\varepsilon_r]$ for uniaxial anisotropic substrate as:

$$[\varepsilon_r]=\begin{bmatrix} \varepsilon_{rt} & 0 & 0 \\ 0 & \varepsilon_{ry} & 0 \\ 0 & 0 & \varepsilon_{rt} \end{bmatrix} \quad \text{with} \quad \varepsilon_{rx}=\varepsilon_{rz}$$

In order to find the dyadic Green's function of the structure, the process starts with the decomposition of the EM field into TM-to-y and TE-to-y waves by introducing coordinate transforms [5] (fig. 1). The vector wave equations for the components of EM field within the uniaxial substrate can be written in their compact form from Maxwell's equations as [6]:

$$\vec{\nabla}\wedge\left(\vec{\nabla}\wedge\vec{E}_i\right)-k_0^2\left[\varepsilon_{ri}\right]\vec{E}_i=0 \qquad (1)$$

$$\vec{\nabla}\wedge\left(\left[\varepsilon_{ri}\right]^{-1}\vec{\nabla}\wedge\vec{H}_i\right)-k_0^2\vec{H}_i=0 \qquad (2)$$

where k_0 is the free-space wave number.

Thus, for the y-components of the EM fields:

$$\frac{\partial^2\widetilde{E}_{yi}}{\partial y^2}+f_{1i}^{\ 2}\widetilde{E}_{yi}=0 \qquad (3.a)$$

$$\frac{\partial^2\widetilde{H}_{yi}}{\partial y^2}+f_{2i}^{\ 2}\widetilde{H}_{yi}=0 \qquad (3.b)$$

with:

$$f_{1i}^{\ 2}=\frac{k_0^2\varepsilon_{ryi}-\alpha_n^2-\beta^2}{\varepsilon_{ryi}}\varepsilon_{ti} \quad \text{and} \quad f_{2i}^{\ 2}=k_0^2\varepsilon_{ti}-\alpha_n^2-\beta^2$$

The solutions of (3.a) and (3.b) are respectively:

$$\widetilde{E}_{yi}=A_i^{TMy}\sinh(f_{1i}(y-H_{i-1}))+B_i^{TMy}\cosh(f_{1i}(y-H_{i-1})) \quad (4.a)$$

$$\widetilde{H}_{yi}=A_i^{TEy}\sinh(f_{2i}(y-H_{i-1}))+B_i^{TEy}\cosh(f_{2i}(y-H_{i-1})) \quad (4.b)$$

where $\gamma_i^{b,a}=\sqrt{\dfrac{-f_{1i}\pm(f_{1i}^2-4f_{2i})^{1/2}}{2}}$

2.1 Derivation of Dyadic Green's function

In this approach, the field formulation for β calculation is bypassed and a direct formulation of the eigenvalue equation is possible without knowledge of the field coefficients (A_i, B_i). All the field components are a superposition of inhomogeneous (in y) plane waves that are propagating in the direction θ of the z-axis, with $\theta=\cos^{-1}(\alpha_n/\delta)$ where $\delta=\sqrt{\alpha_n^2+\beta^2}$. α_n and β are respectively the spectral parameter and the phase constant. For each θ, hybrid waves may be decomposed into TM-to-y and TE-to-y in the (v,y,u) coordinate system.
The tangential components of the EM field are expressed in a dielectric layer i (i = 1,…, N) from Maxwell's equations versus E_y and H_y as:

$$\widetilde{E}_{xi}=-j\alpha_n\frac{\varepsilon_{yi}}{(\alpha_n^2\varepsilon_{xi}+\beta^2\varepsilon_{zi})}\frac{\partial\widetilde{E}_{yi}}{\partial y}+\beta\frac{\omega\mu_0\varepsilon_{zi}}{(\alpha_n^2\varepsilon_{xi}+\beta^2\varepsilon_{zi})}\widetilde{H}_{yi} \quad (5.a)$$

$$\widetilde{E}_z=-j\beta\frac{\varepsilon_{yi}}{(\varepsilon_{zi}\beta^2+\varepsilon_{xi}\alpha_n^2)}\frac{\partial\widetilde{E}_{yi}}{\partial y}-\alpha_n\frac{\omega\mu_0\varepsilon_{xi}}{(\varepsilon_{zi}\beta^2+\varepsilon_{xi}\alpha_n^2)}\widetilde{H}_{yi} \quad (5.b)$$

$$\widetilde{H}_{xi}=-\beta\frac{\omega\varepsilon_{yi}}{(\alpha_n^2+\beta^2)}\widetilde{E}_{yi}-\frac{j\alpha_n}{(\alpha_n^2+\beta^2)}\frac{\partial\widetilde{H}_{yi}}{\partial y} \quad (5.c)$$

$$\widetilde{H}_{zi}=-\frac{j\beta}{(\alpha_n^2+\beta^2)}\frac{\partial\widetilde{H}_{yi}}{\partial y}+\alpha_n\frac{\omega\varepsilon_{22i}}{(\alpha_n^2+\beta^2)}\widetilde{E}_{yi} \quad (5.d)$$

The components of the EM field in the new coordinate system (v,y,u) are deduced via the relations of passage between the two coordinate systems as:

$$\begin{bmatrix} \widetilde{c}_y \\ \widetilde{c}_u \end{bmatrix} = \begin{bmatrix} -\cos\theta & \sin\theta \\ \sin\theta & \cos\theta \end{bmatrix} \begin{bmatrix} \widetilde{c}_x \\ \widetilde{c}_z \end{bmatrix} \quad (c \text{ is E or H}) \qquad (6)$$

where $\cos\theta = \alpha_n/\delta$ and $\sin\theta = \beta/\delta$.

2.1.1. Case of TM$_y$ modes

The boundary conditions on the metallised interface can be expressed in the (v,y,u) coordinate system as:

$$\widetilde{H}_{um+1} - \widetilde{H}_{um} = \widetilde{J}_v \qquad (7.a)$$

$$\widetilde{H}_{vm} - \widetilde{H}_{vm+1} = \widetilde{J}_u \qquad (7.b)$$

$$\widetilde{E}_{um+1} - \widetilde{E}_{um} = 0 \qquad (7.c)$$

$$\widetilde{E}_{vm+1} - \widetilde{E}_{vm} = 0 \qquad (7.d)$$

where $\widetilde{J}_u$ and $\widetilde{J}_v$ are the transformed currents related to $\widetilde{J}_x$ and $\widetilde{J}_z$ via (6). We define the TM$_y$ equivalent admittance seen in the plane of metallisation (at $y=H_m$) by:

$$\widetilde{Y}_v^{TMy} = \frac{\widetilde{J}_v}{\widetilde{E}_{vm}} \qquad (8)$$

Y_v is the input admittance seen in the metallised interface due to all transmission line steps of length h_j [4]. These steps can be terminated by electric walls (Dirichlet's case) or magnetic walls (Neuman's case). Equation (8) can be expressed according to (7.a) and (7.d) as:

$$\widetilde{Y}_v^{TMy} = \widetilde{Y}_{vsup}^{TMy} + \widetilde{Y}_{vinf}^{TMy} \qquad (9)$$

where:

$$\widetilde{Y}_{vsup}^{TMy} = \frac{\widetilde{H}_{u(m+1)}(\alpha_n, H_m)}{\widetilde{E}_{v(m+1)}(\alpha_n, H_m)} \quad \text{and} \quad \widetilde{Y}_{vinf}^{TMy} = \frac{-\widetilde{H}_{um}(\alpha_n, H_m)}{\widetilde{E}_{vm}(\alpha_n, H_m)}$$

Y_{sup} and Y_{inf} are respectively the input admittance seen from top and bottom of the metallised interface (m) Thus, we deduce the equivalent admittance at $y=H_1$ (fig. 1) by:

$$\widetilde{Y}_{v1}^{TMy} = \eta_{v1}^{TMy} \coth(\gamma_1^b H_1) \qquad (10)$$

with:

$$\eta_{v1}^{TMy} = \frac{-j\omega(\varepsilon_x \alpha_n^2 + \varepsilon_z \beta^2)}{\gamma_1^b(\alpha_n^2 + \beta^2)}$$

The parameter η_{v1}^{TMy} can be interpreted as the TM$_y$ characteristic admittance in layer 1 by analogy with the transverse transmission lines. If we generalise to the interface j, one obtain the following recursive process for $\widetilde{Y}_{vinf}^{LSM}$:

$$\widetilde{Y}_{vinf}^{TMy} = \eta_{vj}^{TMy} \frac{\sinh(\gamma_j^a h_j) + S_{vm}^{TMy} \cosh(\gamma_j^b h_j)}{\gamma_j^a \cosh(\gamma_j^a h_j) + \gamma_j^b S_{vj}^{TMy} \sinh(\gamma_m^b h_j)} \qquad (11)$$

with

$$S_{vm}^{TMy} = \frac{B_j}{A_j} = \widetilde{Y}_{v(j-1)}^{TMy} \frac{\gamma_j^a}{\eta_{vj}^{TMy}} \qquad (12)$$

Furthermore, in the plane $(y=H_{N-1})$, we have:

$$\widetilde{Y}_{vN}^{TMy} = -\eta_{vN}^{TMy} \frac{\coth(\gamma_N^b h_N)}{\gamma_N^b}$$

If we generalise to the interface $y=H_m$, one can obtain the following recursive process for $\widetilde{Y}_{vsup}^{TMy}$:

$$\widetilde{Y}_{vsup}^{TMy} = -\eta_{v(j+1)}^{TMy} \frac{\sinh(\gamma_{j+1}^a h_{j+1}) + S_{v(j+1)}^{TMy} \cosh(\gamma_{j+1}^b h_{j+1})}{\gamma_{j+1}^a \cosh(\gamma_{j+1}^a h_{j+1}) + \gamma_{j+1}^b S_{v(j+1)}^{TMy} \sinh(\gamma_{j+1}^b h_{j+1})}$$

$$(13)$$

with :

$$S_{v(j+1)}^{TMy} = -\widetilde{Y}_{v(j+2)}^{TMy} \frac{\gamma_{j+1}^a}{\eta_{v(j+1)}^{TMy}} \qquad (14)$$

$\widetilde{Y}_v^{TMy}$ is obtained by iterating (11) (from j=1 to m) and (13) (from j=m+1 to N) over each section of the transmission line to determine $\widetilde{Y}_{vinf}$ and $\widetilde{Y}_{vsup}$ respectively and summing them.

2.1.2. Case of TE$_y$ modes

We define the TE$_y$ equivalent admittance seen in the metallisation plane $(y=H_m)$ by:

$$\widetilde{Y}_u^{TEy} = \frac{\widetilde{J}_u}{\widetilde{E}_{um}} \qquad (15)$$

which can be written according to (7.b) and (7.c) as:

$$\widetilde{Y}_u^{TEy} = \widetilde{Y}_{usup}^{TEy} + \widetilde{Y}_{uinf}^{TEy}$$

$$\widetilde{Y}_{usup}^{TEy} = \frac{-\widetilde{H}_{v(m+1)}(\alpha_n, H_m)}{\widetilde{E}_{u(m+1)}(\alpha_n, H_m)} \quad \text{and} \quad \widetilde{Y}_{uinf}^{TEy} = \frac{\widetilde{H}_{vm}(\alpha_n, H_m)}{\widetilde{E}_{um}(\alpha_n, H_m)}$$

Otherwise, we have for $\widetilde{Y}_{uinf}^{TEy}$ in the layer 1:

$$\widetilde{Y}_{u1}^{TEy} = \eta_{u1}^{TEy} \coth(\gamma_1^a H_1) \quad \text{with} \quad \eta_{u1}^{TEy} = \frac{j\gamma_1^a}{\omega\mu_0}$$

If we generalise to the interface j, one can obtain the following recursive process for $\widetilde{Y}_{uinf}^{TEy}$:

$$\widetilde{Y}_{uinf}^{TEy}=\eta_{uj}^{LSE}\frac{\gamma_m^a S_{uj}^{TEy}\cosh(\gamma_j^a h_j)+\gamma_j^b \sinh(\gamma_j^b h_j)}{S_{uj}^{TEy}\sinh(\gamma_j^a h_j)+\cosh(\gamma_j^b h_j)} \quad (16)$$

knowing that :

$$S_{uj}^{TEy}=\frac{\widetilde{Y}_{u(j-1)}^{TEy}}{\gamma_j^a \eta_{uj}^{TEy}} \quad (17)$$

By following the same procedure, one can obtain the following recursive process for $\widetilde{Y}_{usup}^{TEy}$:

$$\widetilde{Y}_{usup}^{TEy}=\eta_{u(j+1)}^{TEy}\frac{\gamma_{j+1}^a S_{u(j+1)}^{TEy}\cosh(\gamma_{j+1}^a h_{j+1})+\gamma_{j+1}^b \sinh(\gamma_{j+1}^b h_{j+1})}{S_{u(j+1)}^{TEy}\sinh(\gamma_{j+1}^a h_{j+1})+\cosh(\gamma_{j+1}^b h_{j+1})} \quad (18)$$

with :

$$S_{u(j+1)}^{TEy}=-\frac{\widetilde{Y}_{u(j+2)}^{TEy}}{\gamma_{m+1}^a \eta_{u(j+1)}^{TEy}} \quad (19)$$

$\widetilde{Y}_u^{TEy}$ is obtained by iterating (16) (from j=1 to m) and (18) (from j=m+1 to N) over each section of the transmission line to determine $\widetilde{Y}_{uinf}$ and $\widetilde{Y}_{usup}$, respectively and summing them.

2.2. Deduction of dyadic Green's function

Once the admittance parameters $\widetilde{Y}_u$, $\widetilde{Y}_v$ are known for the TE$_y$ and TM$_y$ modes, the current form is obtained by mapping from (u,v) to (x,z) coordinate system for the spectral wave corresponding to each θ given by α_n and β. The results are as follows:

$$\begin{bmatrix}\widetilde{J}_x(\alpha_n)\\\widetilde{J}_z(\alpha_n)\end{bmatrix}=P\begin{bmatrix}\widetilde{Y}_u^{TEy} & 0\\0 & \widetilde{Y}_v^{TMy}\end{bmatrix}P^{-1}\begin{bmatrix}\widetilde{E}_{x(m+1)}(\alpha_n,H_m)\\\widetilde{E}_{z(m+1)}(\alpha_n,H_m)\end{bmatrix}$$

where P is the matrix of passage between the two coordinate systems which is given by:

$$P=P^{-1}=\begin{bmatrix}-\cos\theta & \sin\theta\\\sin\theta & \cos\theta\end{bmatrix}$$

Finally, a set of matrix equations can be formed yielding the expression for the admittance Green's function:

$$\begin{bmatrix}\widetilde{J}_x(\alpha_n)\\\widetilde{J}_z(\alpha_n)\end{bmatrix}=\begin{bmatrix}\widetilde{Y}_{xx} & \widetilde{Y}_{xz}\\\widetilde{Y}_{zx} & \widetilde{Y}_{zz}\end{bmatrix}\begin{bmatrix}\widetilde{E}_{x(m+1)}(\alpha_n,H_m)\\\widetilde{E}_{z(m+1)}(\alpha_n,H_m)\end{bmatrix} \quad (20)$$

with:

$$\widetilde{Y}_{xx}=\widetilde{Y}_u^{TEy}\cos^2\theta+\widetilde{Y}_v^{TMy}\sin^2\theta$$

$$\widetilde{Y}_{xz}=\widetilde{Y}_{zx}=(\widetilde{Y}_v^{TMy}-\widetilde{Y}_u^{TEy})\cos^2\theta$$

$$\widetilde{Y}_{zz}=\widetilde{Y}_u^{TEy}\sin^2\theta+\widetilde{Y}_v^{TMy}\cos^2\theta$$

The Dyadic Green's function [G] can be deduced simply by inverting the matrix Y. So, the problem of determining [G] reduces to that of finding the admittance parameter Y for the particular structure. This shows the simplicity of applying the spectral domain technique.

3. Application of Galerkin technique

To find the propagation constant, a procedure based on the Galerkin technique is used, by first expanding the unknown currents J_x and J_z of known basis functions (J_{xp} and J_{zq}):

$$\widetilde{J}_x(\alpha_n,\beta)=\sum_{p=1}^{\infty}X_p\widetilde{J}_{xp}(\alpha_n,\beta)$$

$$\widetilde{J}_z(\alpha_n,\beta)=\sum_{q=1}^{\infty}Z_q\widetilde{J}_{zq}(\alpha_n,\beta)$$

and then, substituting $\widetilde{J}_x$ and $\widetilde{J}_z$ into (20) and after taking the inner products with $J_{xp'}$ and $J_{zq'}$, a set of algebraic equations is derived:

$$\sum_{p=1}^{R}C_{pq'}^{11}(\beta)X_p+\sum_{q=1}^{M}C_{qq'}^{12}(\beta)Z_q=0, \quad q'=1..M \quad (21.a)$$

$$\sum_{p=1}^{R}C_{pp'}^{21}(\beta)X_p+\sum_{q=1}^{M}C_{qp'}^{22}(\beta)Z_q=0, \quad p'=1..R \quad (21.b)$$

with:

$$C_{pq'}^{11}(\omega,\beta)=\sum_n G_{11}(\alpha_n)\widetilde{J}_{xp}(x)\widetilde{J}_{zq'}^*(x)$$

$$C_{qq'}^{12}(\omega,\beta)=\sum_n G_{12}(\alpha_n)\widetilde{J}_{zq}(x)\widetilde{J}_{zq'}^*(x)$$

$$C_{pp'}^{21}(\omega,\beta)=\sum_n G_{21}(\alpha_n)\widetilde{J}_{xp}(x)\widetilde{J}_{xp'}^*(x)$$

$$C_{qp'}^{22}(\omega,\beta)=\sum_n G_{22}(\alpha_n)\widetilde{J}_{zq}(x)\widetilde{J}_{xp'}^*(x)$$

The right hands of (21) have been eliminated in the Galerkin process through the application of Parseval's theorem. The simultaneous equations are then solved for the phase constant β by setting the determinant of the coefficient matrix equal to zero and search for the root of the resulting equation.

4. Numerical results

In order to confirm the adequate choice of basis functions, we have analysed the convergence of the effective permittivity of the broadside-inverted microstrip line on boron nitride substrate. Figures 2 and 3 show that 100 Fourier terms and 2 basis functions are sufficient to assure a good convergence. Note also that the narrow lines ($w/h_2 <<1$) require more spectral terms. Therefore, for large bands ($w/h_2 >>1$) the convergence is faster and the CPU time is reduced.
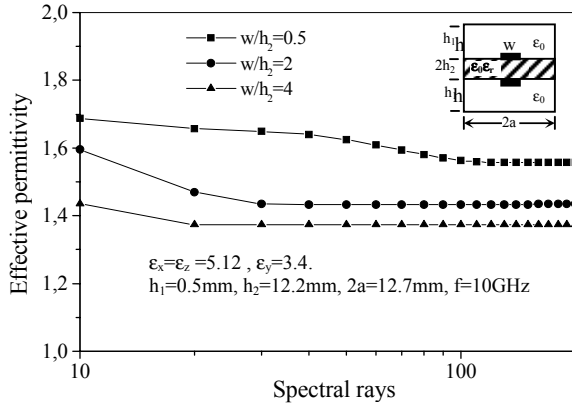
Fig. 2 Convergence of the effective permittivity versus the spectral rays.
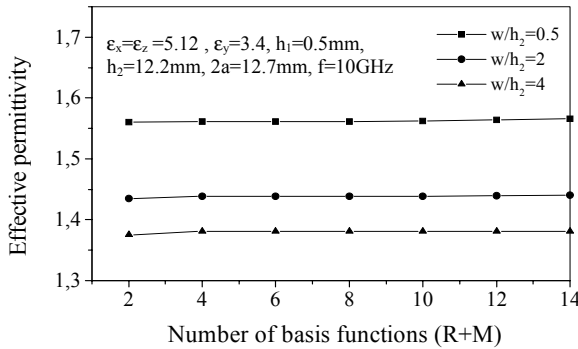
Fig. 3 Convergence of effective permittivity versus the number of basis functions.

Numerical results for lithium niobate are also shown in Fig. 4. In this case, it is quite clear that higher values of the permittivity result in a substantial variation of the propagation constant. Computed results show good agreement with [7].
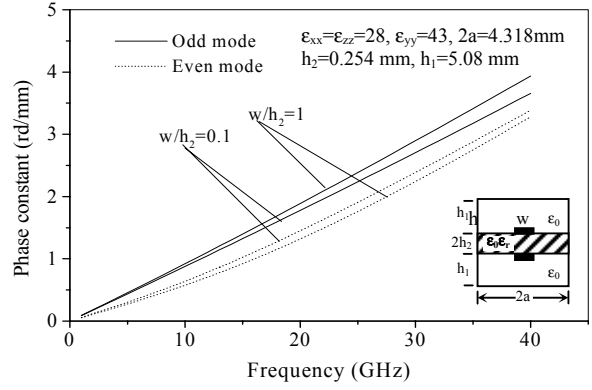
Fig. 4 Dispersion chart of broadside-inverted microstrip line on niobate lithium substrate.

Figures 5 and 6 show the variation of the effective permittivity on boron nitride and saphir substrate respectively. Note that change is negligible over the frequency range from 1 GHz to 30 GHz. The obtained results agree well with [7].
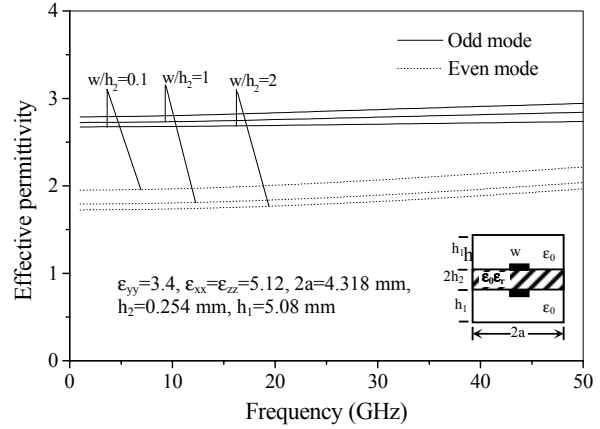
Fig. 5 Effective permittivity of broadside-inverted coupled microstrip line on boron nitride substrate.
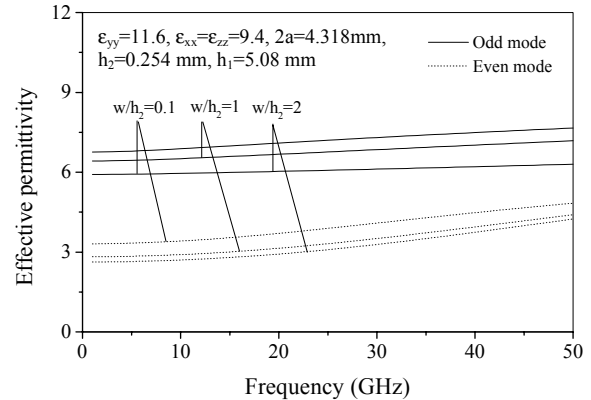
Fig. 6 Effective permittivity of broadside-inverted coupled microstrip line on saphir substrate.

This low dispersion feature signifies the fact that the quasi-static analysis is adequate for designing practical microwave and millimeter-wave circuits. In this case, the modeling of the structure in quasi-static mode would require less efforts of computation with consequently reduced CPU times.

Figures 7 (a-b) illustrate the variation of effective permittivity for broadside edge-coupled structures printed on Epsilam 10 substrate. Note that the even-even and odd-even modes are relatively insensitive to the dispersion phenomenon in contrast to the even-odd and odd-odd modes where the dispersion is significant particularly for large strips (w/b >>1).

(a)

(b)
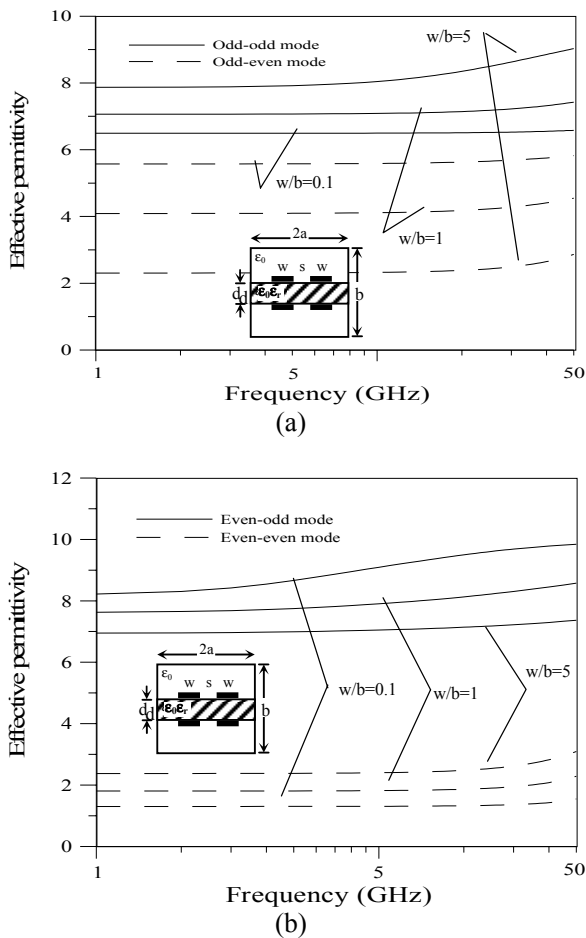
Fig. 7 Effective permittivity versus frequency of broadside edge-coupled inverted microstrip line on Epsilam 10 substrate. a)- For odd-odd and odd-even modes, b)- For even-odd and even-even modes.

Note also that the values of the effective permittivity for odd-even and even-even modes decreases versus w/b but increases for the two other modes.

5. Conclusion

In this paper, the dispersion characteristics of the multilayered bilateral microwave structures with uniaxial anisotropic substrate have been formulated using the spectral domain technique. The Galerkin method was employed to find the propagation constant. Numerical results for effective dielectric constants and dispersion charts have been presented, including the convergence behaviour.

It has been found that broadside-microstrip structures present very small dispersion, which confirms the adequacy of the quasi-static analysis for high-frequency circuit design purposes. This weak dispersion, together with the inherent features of broadband, tigh-coupling and large mode velocity ratio, makes the broadside-coupled structure very attractive for MIC and MMIC applications.

References:
[1] A. Alu, F. Bilotti and L. Vegni, "Generalized transmission line equations for bianisotropic materials," *IEEE Transactions on Antennas and Propagation*, vol. 51, 2003, pp. 3134-3141.
[2] M.L. Tounsi, A. Khodja and M.C.E. Yagoub, " Efficient analysis of multilayered broadside edge-coupled anisotropic structures for microwave applications", *IEEE International Symposium on Circuits and Systems,* vol. IV, pp. 229-232, 2004,
[3] A. Alu, F. Bilotti and L. Vegni, "Extended method of line procedure for the analysis of microwave components with bianisotropic inhomogeneous media," *IEEE Transactions on Antennas and Propagation*, vol. 51, 2003, pp. 1582 - 1589
[4] T. Uwano and T. Itoh, "Spectral domain approach," *in Numerical techniques for microwave and millimeter-wave passive structures*, T. Itoh, Ed. New York Wiley, 1989.
[5] T. Itoh, "Spectral domain immitance approach for dispersion characteristics of generalized printed transmission lines"*, IEEE Trans. Microwave Theory Tech.*, vol. 28, 1980, pp. 733-736.
[6] Y. Chen and B. Beker, "Analysis of single and coupled microstrip lines on anisotropic substrate using differential matrix operators and spectral domain method", *IEEE Trans. Microwave Theory Tech.*, vol. 41, Jan. 1993, pp. 123-128.
[7] T.Q. Ho and B. Beker "Frequency-dependent characteristics of shielded broadside microstrip lines on anisotropic substrates," *IEEE Trans. Microwave Theory Tech.*, vol. 39, 1991, pp. 1021-1025.